Cancer Research

The Small Molecule IMR-1 Inhibits the Notch Transcriptional Activation Complex to Suppress Tumorigenesis

Luisana Astudillo[1,2], Thiago G. Da Silva[1,2], Zhiqiang Wang[1,2], Xiaoqing Han[1,2], Ke Jin[1,2], Jeffrey VanWye[1,2], Xiaoxia Zhu[1,2], Kelly Weaver[1,2], Taiji Oashi[3], Pedro E.M. Lopes[3], Darren Orton[4], Leif R. Neitzel[5], Ethan Lee[5], Ralf Landgraf[2,6], David J. Robbins[1,2], Alexander D. MacKerellJr[3], and Anthony J. Capobianco[1,2]

Abstract

In many cancers, aberrant Notch activity has been demonstrated to play a role in the initiation and maintenance of the neoplastic phenotype and in cancer stem cells, which may allude to its additional involvement in metastasis and resistance to therapy. Therefore, Notch is an exceedingly attractive therapeutic target in cancer, but the full range of potential targets within the pathway has been underexplored. To date, there are no small-molecule inhibitors that directly target the intracellular Notch pathway or the assembly of the transcriptional activation complex. Here, we describe an *in vitro* assay that quantitatively measures the assembly of the Notch transcriptional complex on DNA. Integrating this approach with computer-aided drug design, we explored potential ligand-binding sites and screened for compounds that could disrupt the assembly of the Notch transcriptional activation complex. We identified a small-molecule inhibitor, termed Inhibitor of Mastermind Recruitment-1 (IMR-1), that disrupted the recruitment of Mastermind-like 1 to the Notch transcriptional activation complex on chromatin, thereby attenuating Notch target gene transcription. Furthermore, IMR-1 inhibited the growth of Notch-dependent cell lines and significantly abrogated the growth of patient-derived tumor xenografts. Taken together, our findings suggest that a novel class of Notch inhibitors targeting the transcriptional activation complex may represent a new paradigm for Notch-based anticancer therapeutics, warranting further preclinical characterization. *Cancer Res; 76(12); 3593–603. ©2016 AACR.*

Introduction

The promise of precision treatment for cancer is predicated on the assumption that a comprehensive array of targeted therapeutics will be available in the future. Therefore, there is a substantial unmet need to identify and successfully drug not only the drivers but also the signaling pathways that are critical for the maintenance of the neoplastic phenotype. Furthermore, there is a need for therapeutic depth in these critical pathways to overcome acquired resistance. However, the number of "druggable" targets is finite, which represents a potential hurdle to personalized medicine. As most proteins function in higher order complexes mediated by protein–protein interactions, targeting these interactions represents a broad range of potential targets and therapeutics to be explored.

The Notch pathway is widely utilized in development to govern cell fate specification and to balance proliferative capacity and differentiation state (1, 2). In the adult, the Notch pathway is restricted to small populations of progenitor and stem cells of regenerating tissues such as the colon and brain (3, 4). However, in many human cancers, the Notch pathway becomes reactivated (for review, see ref. 5). The deregulation of the Notch pathway underlies many aspects of cancer physiology in a cell type- and context-dependent manner (5–7). Aberrant Notch activity has been demonstrated to play a role in the initiation and maintenance of the neoplastic phenotype as well as playing a central role in cancer stem cells, thereby underlying a role in metastasis and resistance to therapy (8, 9).

Notch drives a context-dependent cellular response by initiating and maintaining a transcriptional cascade (10, 11). This transcriptional response is mediated by Notch by directing the formation of a core transcriptional activation complex, termed the Notch ternary complex (NTC). The NTC comprises the DNA-binding protein CSL [CBF-1/RBP-J, Su(H), Lag-1], the intracellular domain of Notch (NICD), and the coactivator protein Mastermind-like 1 (Maml1; refs. 12–14). Current approaches to inhibit the Notch pathway include mAbs that target and disrupt

[1]Molecular Oncology Program, Division of Surgical Oncology, Dewitt Daughtry Family Department of Surgery, University of Miami, Miami, Florida. [2]Sylvester Comprehensive Cancer Center, Miller School of Medicine, University of Miami, Miami, Florida. [3]Department of Pharmaceutical Sciences, School of Pharmacy, University of Maryland, Baltimore, Maryland. [4]StemSynergy Therapeutics, Inc., Miami, Florida. [5]Department of Cell and Developmental Biology and Ingram Cancer Center, Vanderbilt University Medical Center, Nashville, Tennessee. [6]Department of Biochemistry and Molecular Biology, University of Miami, Miami, Florida.

Note: Supplementary data for this article are available at Cancer Research Online (http://cancerres.aacrjournals.org/).

L. Astudillo and T.G. Da Silva contributed equally as first authors. Z. Wang, X. Han, K. Jin and J. Vanwye contributed equally as second authors.

Corresponding Author: Anthony J. Capobianco, University of Miami, 1600 NW 10th Avenue, RMSB 1040 (R-104), Miami, FL 33136. Phone: 305-243-6308; Fax: 305-243-8039; E-mail: tcapobianco@med.miami.edu

doi: 10.1158/0008-5472.CAN-16-0061

Notch–ligand interactions or small-molecule inhibition of the presenilin-dependent γ-secretase (γ-secretase inhibitors, GSI; refs. 15–21). Both of these approaches serve to block ligand-dependent production of NICD, acting at the top of the Notch signaling cascade. Alternatively, truncated forms of Maml1 have been demonstrated to act in a dominant negative manner in the Notch pathway (13, 22–26). Along these lines, Moellering and colleagues designed and synthesized a peptide derived from Maml1, termed SAHM1 (stapled α-helical peptide derived from Maml1), which competes with Maml1 and inhibits the formation of the NTC (27). Therefore, SAHM1 functions as a dominant negative inhibitor (27). Although this approach worked at a scale feasible for mouse studies, the use of peptides as therapeutics still face significant challenges, whereas small-molecule inhibitors represent a more desirable approach for cancer therapeutics. However, to date there are no small-molecule inhibitors of the transcriptional activation complex or that are specific to the Notch pathway itself.

Herein, we present proof-of-concept for a first-in-class inhibitor of the Notch transcriptional activation complex. We describe the identification and validation of a small-molecule inhibitor of Mastermind recruitment-1 (IMR-1) to the Notch transcriptional activation complex. We demonstrate that IMR-1 prevents the recruitment of Maml1 to the NTC on chromatin, inhibits Notch target gene transcription, and dramatically inhibits tumor growth in a patient-derived tumor xenograft model.

Materials and Methods

Compounds

Compounds were purchased from ChemDiv, ChemBridge, or SPECS (the Netherlands). Catalog numbers and chemical details are available upon request.

Cell lines

OE19 and OE33 human esophageal adenocarcinoma cell lines were obtained from the European Collection of Cell Culture. SUM-149 and SUM-159 (human ER^- basal breast cancer) were obtained from Dr. Joyce Slingerland at the University of Miami, Miller School of Medicine (Miami, FL). Cell lines 786-0 (human renal adenocarcinoma), HT-1080 (human fibrosarcoma), MCF-7, and T47D (ER^+ luminal breast cancer), and H-23 (non–small cell lung adenocarcinoma) were obtained from ATCC. All cell lines were tested for mycoplasma contamination and propagated in growth media as specified by the provider. Cell lines were obtained between 2008 and 2015 and authenticated by ATCC (cell line authentication profiling utilizing short tandem repeat profiling).

Notch complex assembly assay

Recombinant proteins were expressed using baculovirus expression vectors in SF21 cells and purified as described previously (13, 28). Unless otherwise stated, all assays contained 125 fmol of double-stranded (DS) oligonucleotide, CSL, Notch, and Maml1 proteins in TBS-T buffer containing 0.2% BSA and 100 μg/mL salmon sperm DNA. Briefly, the Notch complex was assembled on a biotinylated DS oligonucleotide harboring one CSL binding site (5′-AAACACGCCGTGGGAAAAAATTTATG-3′). Complex assembly was quantitated using AlphaScreen technology on an Envision plate reader (Perkin Elmer), following manufacturer's instructions. Proteins in the complex were detected using specific antibodies to either Maml1 (Cell Signaling Technology; D3K7B), Notch1 (Abcam, 52627), or CSL (anti-His, Abcam, 18184). Streptavidin-conjugated donor beads (Perkin Elmer) were used to bind the DS oligonucleotide and Protein-A–conjugated acceptor beads (Perkin Elmer) to detect antibody-coated proteins. NTC components were added to wells containing the small molecules to be assayed and incubated for 30 minutes. Acceptor beads and the antibody specific for Maml1, Notch1, or CSL were then added to the reaction mixture and incubated in the dark for 30 minutes, followed by addition of the donor beads and incubated in the dark for 1 hour. Assays were performed in 384-well plates in triplicate (AlphaScreen plate; Perkin Elmer). Data analysis was performed using GraphPad Prism software (Version 5).

Western blot analysis

Protein analysis was performed as previously described (28) using anti-Notch1 (Abcam, ab52627), anti-$Notch1^{val1744}$ (Cell Signaling Technology, 4147S), and anti-GAPDH (Abcam, ab9483) antibodies.

Real-time qPCR analysis

Reverse transcription and qPCR analysis were performed as described previously (28). Gene expression was normalized to *TBP* and *HPRT*. TaqMan primer sequences are available upon request.

DNA pulldown

DNA pulldown was performed as previously described (28). 293T cells were transfected with Maml1, NICD, and NICD single mutants (R2096, R2105, R2061, and R2071) using LipoJet *In Vitro* Transfection Kit (SignaGen Laboratories). Proteins bound to the beads were analyzed by Western blotting.

Surface plasmon resonance

Notch1 was covalently immobilized to the sensor chip surface (CM5 chip, GE) by standard amine coupling (29). Experiments were performed on a Biacore T200 instrument (GE Healthcare) at 25°C using PBS (10 mmol/L, pH 7.5) containing 5% DMSO as running buffer. The sample SPR signal was corrected with its respective control containing DMSO. Data visualization and analysis were performed using Biacore T200 software (GE Healthcare) and Origin 8.0 (OriginLab).

Statistical analysis

P value was calculated using χ^2 in contingency table. The sample size was chosen to be greater than the minimal sample size from power assessment as described previously (30). Data are presented as mean ± SEM and were analyzed by two-tailed Student *t* test. A *P* value of less than 0.05 was considered significant.

Results

Computer-aided drug design of CSL–Notch1 interface inhibitors

Assembly of the Notch transcriptional activation complex is thought to occur in a stepwise fashion (13, 28, 31, 32). The crystal structure of the NTC (PDB ID: 2F8X) shows a protein–protein interface between the ANK repeat domain of Notch1 and CSL that could act as a binding site for small molecules. Notch1 and CSL create a cleft required for stable Maml1 association to the

complex. Once bound, Maml1 locks the core scaffold together and serves to recruit the higher order transcription regulatory machinery, thereby initiating the expression of Notch target genes (12, 28, 33). We reasoned that CSL–Notch1 interactions could be disrupted upon small-molecule binding, thus preventing Maml1 recruitment and leading to inhibition of NTC assembly. Because Maml1 is critical to Notch activity (27), compounds that prevent Maml1 recruitment would potentially inhibit Notch transcriptional activation. Therefore, to identify compounds that could inhibit the NTC assembly, we performed *in silico* analysis of the NTC structure to obtain structural variability for the initial screening of a large database of small molecules. We utilized eight representative structures of the NTC core complex that were generated using molecular dynamics (MD) simulations and the X-ray crystallographic structure. Sites on the NTC were evaluated by docking 1,000 chemically distinct probe molecules and calculating the binding response (BR) score, which is based on energetic and geometric criteria (34). A common site on the ANK repeat domain of Notch1 was identified on seven of the MD conformations and the crystal conformation, yielding a total of eight conformations for screening. This site is composed of residues that span the fourth through seventh ankyrin repeats of Notch1. Primary *in silico* screening of this pocket was performed on an in-house database (>1.5 million commercially available drug-like small molecules). Each ligand was docked into the putative binding site for each protein conformation using the program DOCK (35) and a score was assigned on the basis of the most favorable normalized van der Waals (vdW) attractive energy among all the protein conformations. A secondary screening of the top 50,000 molecules selected from the primary screens involved more rigorous optimization during docking. Each compound was docked individually against each of the eight protein conformations with the most favorable normalized total interaction energy over all the conformations taken as the score for each compound. The top scoring 1,000 compounds were selected. The final compounds for experimental evaluation were chosen based on their chemical diversity to maximize the possibility of identifying unique leads for further optimization and development and on their physicochemical properties to maximize their potential bioavailability (36). We selected 150 compounds that were obtained from commercial vendors for testing.

Development of a Notch ternary complex assembly assay

We developed an *in vitro* assay that quantitatively measures the assembly of the NTC on DNA to screen for compounds that could inhibit NTC formation. Briefly, baculovirus-produced CSL, Notch1, and Maml1 are used to build the NTC on a biotinylated oligonucleotide scaffold that harbors a CSL binding site. A Maml1-specific antibody is used to detect recruitment of Maml1 to the complex on DNA and complex formation is then detected with the proximity-based AlphaScreen technology (Perkin Elmer) using streptavidin donor and protein A acceptor beads (Fig. 1A). Therefore, a signal should only be generated when Maml1 is recruited to CSL on DNA. To demonstrate that the signal observed resulted from the recruitment of Maml1 to the complex, Maml1 was titrated against a fixed amount of the remaining reaction components. A dose-dependent increase in signal was observed upon Maml1 addition up to the stoichiometric equivalence point (250 fmol, Fig. 1B, left). Similar results were observed upon titration of Notch1 (Fig. 1B, right), indicating that recruitment of Maml1 depends on Notch1 binding to CSL. Furthermore, complex assembly is dependent on CSL binding to DNA, because an oligonucleotide that harbors a mutant CSL–binding site does not generate an appreciable signal (Fig. 1C, shaded area).

To further authenticate the *in vitro* NTC assembly assay, we probed different components and conditions to determine whether the assay recapitulates established parameters of the NTC on DNA. As previously described for Maml1 (Fig. 1B, left), a signal is only observed when all components of the NTC are present in the reaction (Fig. 1D, lanes 1–5). No signal is observed when either CSL or Notch1 is absent from the reaction (Fig. 1D, lanes 6 and 7), indicating that binding of Maml1 to the complex requires both CSL and Notch1. Furthermore, CSL binds to DNA in the absence of the other NTC components (Fig. 1D, lanes 16–19), whereas Notch1 requires CSL, but not Maml1, to bind to DNA (Fig. 1D, lanes 11–13). We also tested the requirement of specific protein domains (37). Deletion of the Notch RAM domain caused a loss in the binding of both Notch1 and Maml1 to the complex (Fig. 1D, lanes 9 and 15), whereas deletion of the Notch PEST domain did not alter the assembly of the NTC (Fig. 1D, lanes 8 and 14). The results described here demonstrate that the assay measures the assembly of a *bona fide* NTC, as the recruitment of Maml1 to the NTC is dependent on the high affinity binding of Notch1 to CSL through its RAM domain.

Screening of small-molecule inhibitors of the NTC led to the identification of IMR-1

The *in vitro* NTC assay was utilized to screen small molecules derived from computer-aided drug design (CADD). From the 150 compounds tested, 30 compounds showed a decrease in Maml1 recruitment of at least 50% compared with the positive control (all components of the NTC; Supplementary Fig. S1A). In particular, three compounds showed remarkable inhibitory activity (>90%), and compound 1-134 inhibited assembly by 97% (Supplementary Fig. S1A, shaded area). To obtain structural variability and validate these results, the scaffold of 1-134 was subjected to *in silico* similarity search (38) using a virtual 2D database. Fifty-four of the 1-134 derivative compounds were commercially available and tested at 30 μmol/L. Only 16 compounds inhibited complex assembly by more than 50% (Supplementary Fig. S1B). These compounds were counter-screened against Notch1 and CSL antibodies using the *in vitro* NTC assembly assay to demonstrate their specificity at displacing Maml1 from the complex. The data indicate that the 1-134 derivatives did not displace CSL or Notch1 from the complex (Supplementary Fig. S1C, white bars and striped bars, respectively). Therefore, the 1-134 derivatives specifically disrupt the binding of Maml1 to the NTC *in vitro*. To better evaluate the potency of these compounds, the *in vitro* NTC assay was used to generate dose–response curves and determine their IC_{50}.

The core molecular scaffold of 1-134 and its derivatives is a thiazolidinone consisting of a phenyl ring and a rhodanine moiety connected by a double bond. Dose–response curves of 1-134 and its 16 prioritized analogues indicated that the parent compound 1-134 showed promising *in vitro* potency (IC_{50} = 6 μmol/L) in the NTC assay. The rhodanine ester compound (1-134-83, termed IMR-1) exhibited an IC_{50} of 26 μmol/L (Fig. 1E), whereas the other compounds exhibited IC_{50} greater than 26 μmol/L (data not shown). Because ester containing compounds may undergo hydrolysis *in vivo* by the action of several esterases (39), we also tested the acid metabolite of IMR-1 (compound

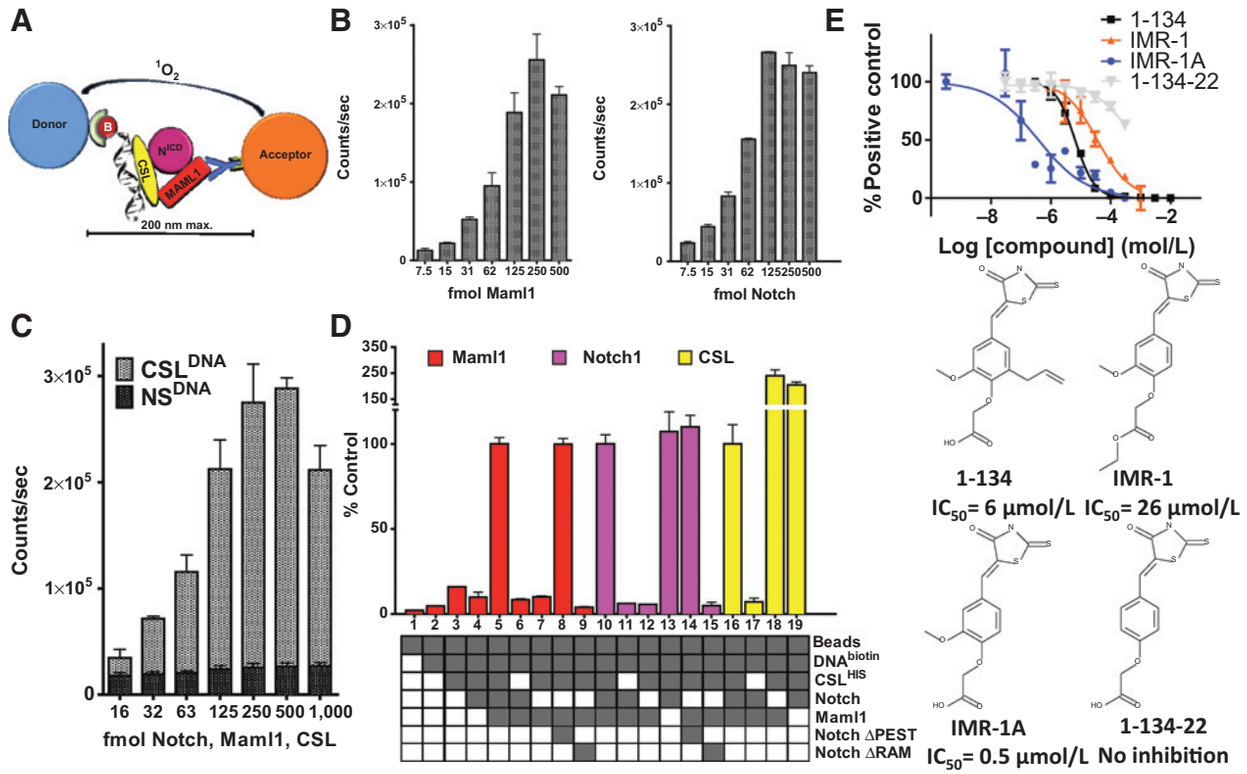

Figure 1.
The NTC assembly assay. A, schematic representation of the *in vitro* NTC assay. B, titration of Maml1 (left) and NICD (right) in NTC assay. C, NTC assay requires an intact CSL consensus site. CSL^{DNA} represents an oligonucleotide harboring the CSL consensus sequence, whereas NS^{DNA} represents an oligonucleotide that harbors a mutant CSL–binding site. D, NTC assay represents a *bona fide* Notch ternary complex. Colors denote probes for specific components: anti-Maml1–specific Ab, red; anti-Notch1–specific Ab, purple; anti-His Tag Ab-specific for His-tagged CSL, yellow. Box grid indicates components present (shaded) in the reactions. E, IC_{50} determination for compounds 1-134, IMR-1, IMR-1A, and 1-134-22 and corresponding structures (bottom).

IMR-1A) and observed a 50-fold increase in potency for IMR-1A ($IC_{50} = 0.5$ μmol/L) with respect to IMR-1. Interestingly, removal of the methoxy group of 1-134-2, corresponding to compound 1-134-22 (Fig. 1E), leads to no inhibition of NTC formation as evident by the large concentration of 1-134-22 required to observe a small decrease in signal in the *in vitro* NTC assay (Fig. 1E). These results also suggest a role of the methoxy group at this position in binding to the target protein(s).

IMR-1 demonstrates noncovalent binding to Notch1 with micromolar affinity

To determine the affinity of small-molecule inhibitors of the NTC for Notch1 and characterize their molecular interactions, we used surface plasmon resonance (SPR). Representative sensorgrams determined for the association of 1-134, IMR-1, and IMR-1A to NICD are presented in Fig. 2A–C. The dissociation constants associated with binding of the compounds to NICD was determined using the equilibrium approach by plotting the equilibrium response (R_{eq}) as a function of the compound concentration and fitting the data to a 1:1 binding model (Fig. 2D). Compound 1-134 binds with moderate affinity to NICD ($K_D = 17 \pm 5$ μmol/L). A slightly higher affinity was observed for IMR-1 ($K_D = 11 \pm 3$ μmol/L), whereas a significantly higher affinity to NICD was observed for IMR-1A ($K_D = 2.9 \pm 0.6$ μmol/L). Noteworthy, the SPR sensorgrams measured for association of 1-134, IMR-1, and IMR-1A indicate noncovalent, reversible binding to Notch1 as evident by the dissociation curves reaching baseline upon introduction of buffer solution with a rate constant within the range of small-molecule dissociation from proteins (Fig. 2A–C).

To obtain insight into the molecular interactions between IMR-1 and the NTC and assessment of the binding site, we performed molecular docking simulations of the inhibitors to the NTC (PDB file: 2F8X). The data suggested that residues from ANK (R2096, R2105, R2061, and R2071) were located within the binding pocket. To determine the effect of each residue on the binding of IMR-1 to Notch1, the affinity of NTC inhibitors to wild-type (WT) NICD and single-point mutated NICD (R2096A, R2105A, R2061A, and R2071A) was determined by SPR. Replacement of R2061 and R2071 with alanine decreases the affinity of IMR-1 to NICD by approximately fivefold (K_D of 35.6 and 38.7 μmol/L, respectively; Fig. 2E). No effect was observed upon substitution of R2096 and R2105 by alanine. These results suggest that R2061 and R2071 play an intimate role in the binding of IMR-1 to NICD. Docking of IMR-1 to the NTC suggests that IMR-1 interacts with Notch1 and CSL residues (Fig. 2F). CSL residues interacting with IMR-1 include Q362, N363, G384, and M126. In addition, the carbonyl group from the ester moiety of IMR-1 interacts with one of the –NH groups from the side chain of R2061 from Notch1 through hydrogen bonding, consistent with the lower affinity of IMR-1 to R2061A (Fig. 2E). The docking model also suggests that R2071 (Notch1) is located in close proximity to IMR-1 (Fig. 2F) and may be involved in long-range interactions with IMR-1,

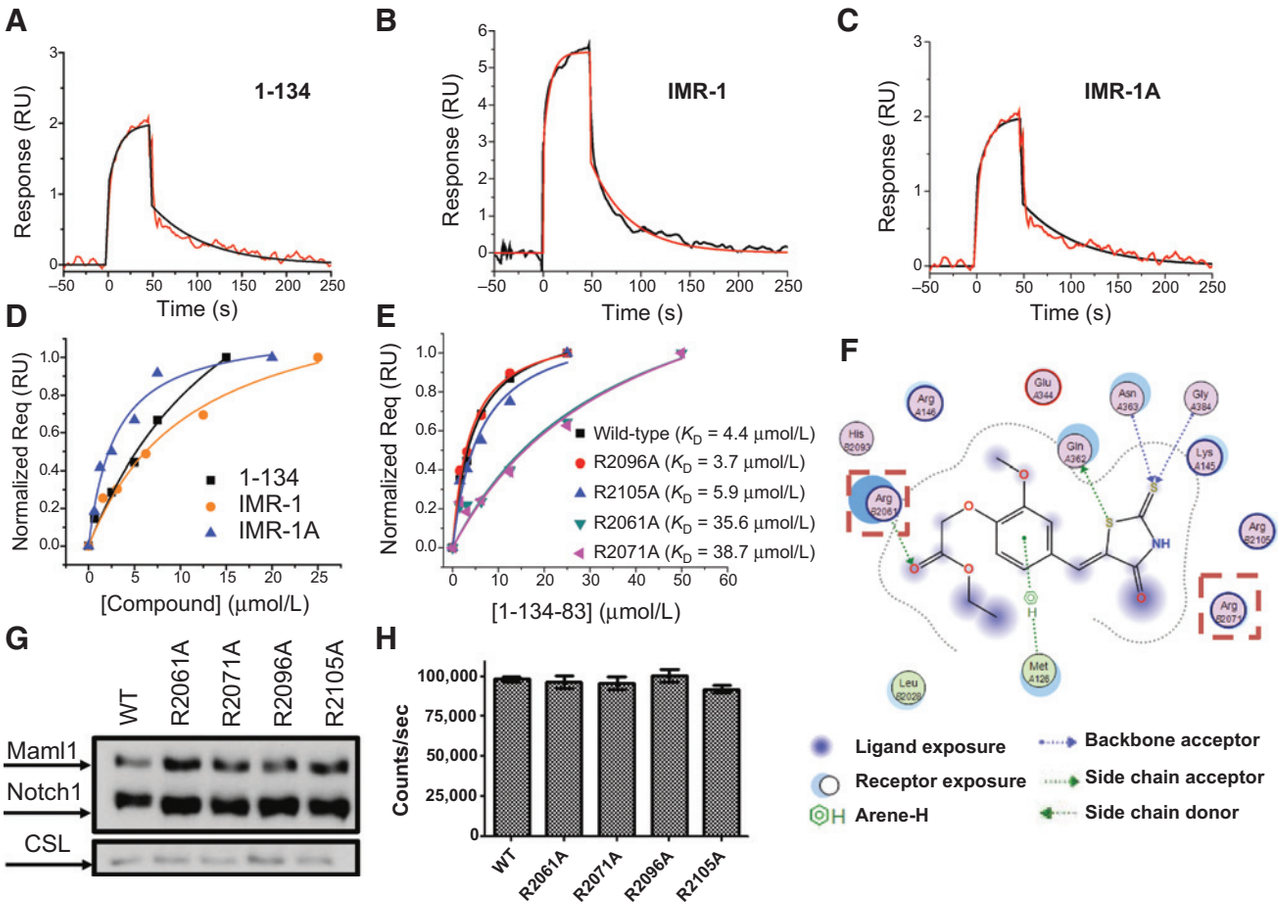

Figure 2.
Affinity of NTC inhibitors to Notch1. A–C, sensorgrams determined for 1-134 (A), IMR-1 (B), and IMR-1A (C) binding to NICD. D, dose–response curves of 1-134, IMR-1, and IMR-1A to NICD determined by SPR. E, affinity of IMR-1 to NICD and mutants determined by SPR. F, docking model of IMR-1 binding to the NTC. Arginine residues located in the binding pocket of IMR-1 are enclosed in red boxes. DNA pull-down (G) in 293T cells and NTC assay (H) with NICD and single arginine mutated NICD demonstrate no effect of single mutations on NTC assembly.

which would explain the decrease in affinity of IMR-1 to R2071A. To determine whether these mutations affect the ability of Notch1 to form the NTC, we analyzed complex formation by DNA pulldown and the *in vitro* NTC assay. DNA pulldown on CSL oligonucleotide beads (Fig. 2G) and the NTC assay (Fig. 2H) demonstrates mutated NICD proteins retain the ability to form the ternary complex, as evident by the similar signal observed between the WT and mutated NICD proteins.

IMR-1 inhibits Notch target gene transcription by disrupting Maml1 recruitment to chromatin

Once we established that the CADD-derived compounds specifically disrupt the recruitment of Maml1 to the activation complex *in vitro*, we sought to determine whether 1-134 and its 16 prioritized derivatives exhibit biologic activity using a cell-based assay. A colony formation assay was used a secondary screening to test biologic activity. To this end, cell lines selected for screening were classified into two groups based on their sensitivity to DAPT (a GSI), to establish a criterion for Notch dependence. We reasoned that inhibition of cell growth and gene transcription by DAPT indicates specific inhibition of Notch activity. Therefore, cell lines exhibiting inhibition of growth and transcription of Notch target genes upon treatment with DAPT were classified as Notch dependent, whereas those in which transcription and growth did not significantly change upon DAPT treatment were classified as Notch-independent cell lines. A decrease in colony formation of Notch-dependent cell lines is observed upon treatment with IMR-1 when compared with the control (DMSO). However, no effect was observed for 1-134 and its other derivatives up to concentrations of 30 to 45 μmol/L (data not shown), likely due to low cell permeability. Therefore, IMR-1 was prioritized for further testing.

To determine the effect of IMR-1 treatment on the assembly of the NTC in cells, Notch-dependent cell lines OE33 and 786-0 were treated with DAPT or IMR-1. Treatment with DAPT decreased the occupancy of Notch and Maml1 on the *HES1* promoter using a chromatin immunoprecipitation (ChIP) assay (Fig. 3A). This effect is caused by a decrease in the NICD pool due to the inhibition of presenilin-dependent γ-secretase. Treatment of OE33 and 786-0 with IMR-1 also decreased the occupancy of Maml1 on the *HES1* promoter but, in contrast to DAPT treatment, IMR-1 treatment did not affect the occupancy of Notch1 on the *HES1* promoter (Fig. 3A). Western blot analysis of the lysates demonstrates that IMR-1 treatment does not change the levels of

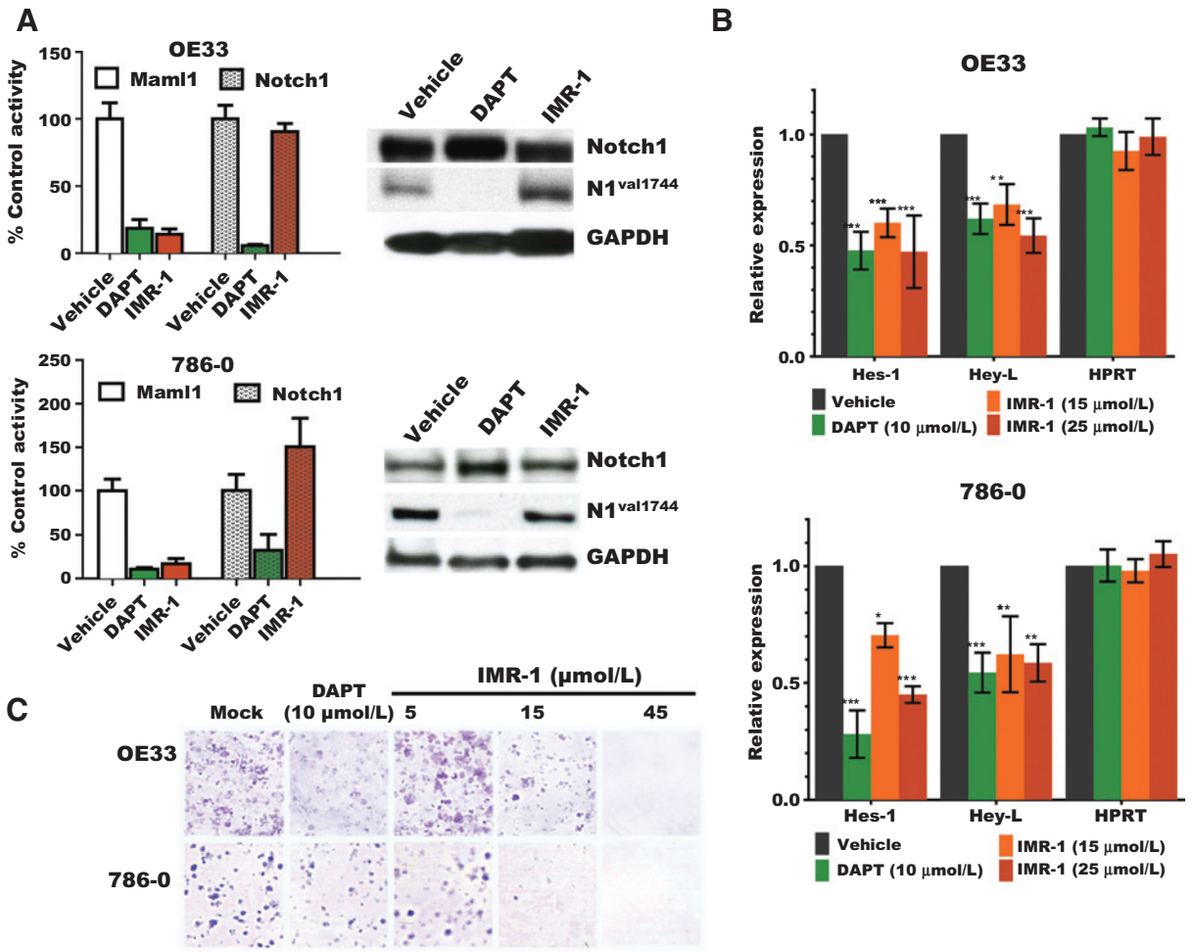

Figure 3.
IMR-1 is an inhibitor of the Notch transcriptional activation complex. A, ChIP assay on the *HES1* promoter using the indicated antibodies (left) following treatment of OE33 (top) and 786-0 cells (bottom) with DAPT (15 μmol/L), IMR-1 (25 μmol/L), or vehicle (DMSO) using GAPDH as loading control. Western blot analysis of Notch1 and cleaved Notch1 ($N1^{Val1744}$) from cells used in ChIP assay (right). B, RT-qPCR analysis of Notch target genes (Hes-1, Hey-L) in treated OE33 and 786-0 cells (control gene: HPRT). Data are expressed as relative expression to vehicle control (set to 1). C, colony formation assay in Notch-dependent cell lines (OE33 and 786-0).

NICD in cells (Fig. 3A, right). Therefore, these data indicate that IMR-1 specifically disrupts the recruitment of Maml1 to chromatin while the binding of NICD to CSL is unaffected. As IMR-1 treatment leads to disruption of the NTC on chromatin, we sought to determine whether IMR-1 also abrogates Notch target gene transcription (Fig. 3B). IMR-1–treated cells displayed a dose-dependent decrease in Notch target gene transcription similar to the control cells treated with DAPT. As proof of specificity, transcription of the housekeeping gene *HPRT* was unaltered in treated cells. To test the effects of Notch inhibition on proliferation, we performed a colony formation assay. Treatment of cells with IMR-1 displayed a dose-dependent reduction in colony formation in both 786-0 and OE33 cell lines (Fig. 3C). To extend the analysis of tumor cell growth inhibition, we selected several commonly used cancer cell lines to test for sensitivity to IMR-1 (Fig. 4A). The sensitivity profile for cells treated with either IMR-1 or DAPT was comparable, indicating that IMR-1 is specifically inhibiting Notch activity (Fig. 4A). Colony formation displayed a similar stratification, that is, cells with transcriptional sensitivity to IMR-1 and DAPT treatment exhibited impaired colony-forming ability (Fig. 4B). Cells that are refractory to DAPT were equally resistant to IMR-1. Taken together, these data indicate that IMR-1 selectively affect Notch-dependent cell lines via the inhibition of Notch-directed transcriptional activation by blocking the recruitment of Mam1 to the Notch transcriptional complex on chromatin.

IMR-1 inhibits xenograft tumor growth

To determine the effect of IMR-1 on tumor formation in an animal model of cancer, we utilized an established xenograft model (40). When introduced into the flank of a nude mouse, 5×10^6 OE19 human esophageal adenocarcinoma cells readily form tumors over the course of 4 weeks. Treatment of these mice with 15 mg/kg IMR-1 readily blocks tumor establishment. In contrast, treatment with DMSO (control) had no effect on tumor growth (Supplementary Fig. S2). IMR-1 treatment at 15 mg/kg caused no observable adverse effects on the animal and body weight remained constant throughout the treatment course

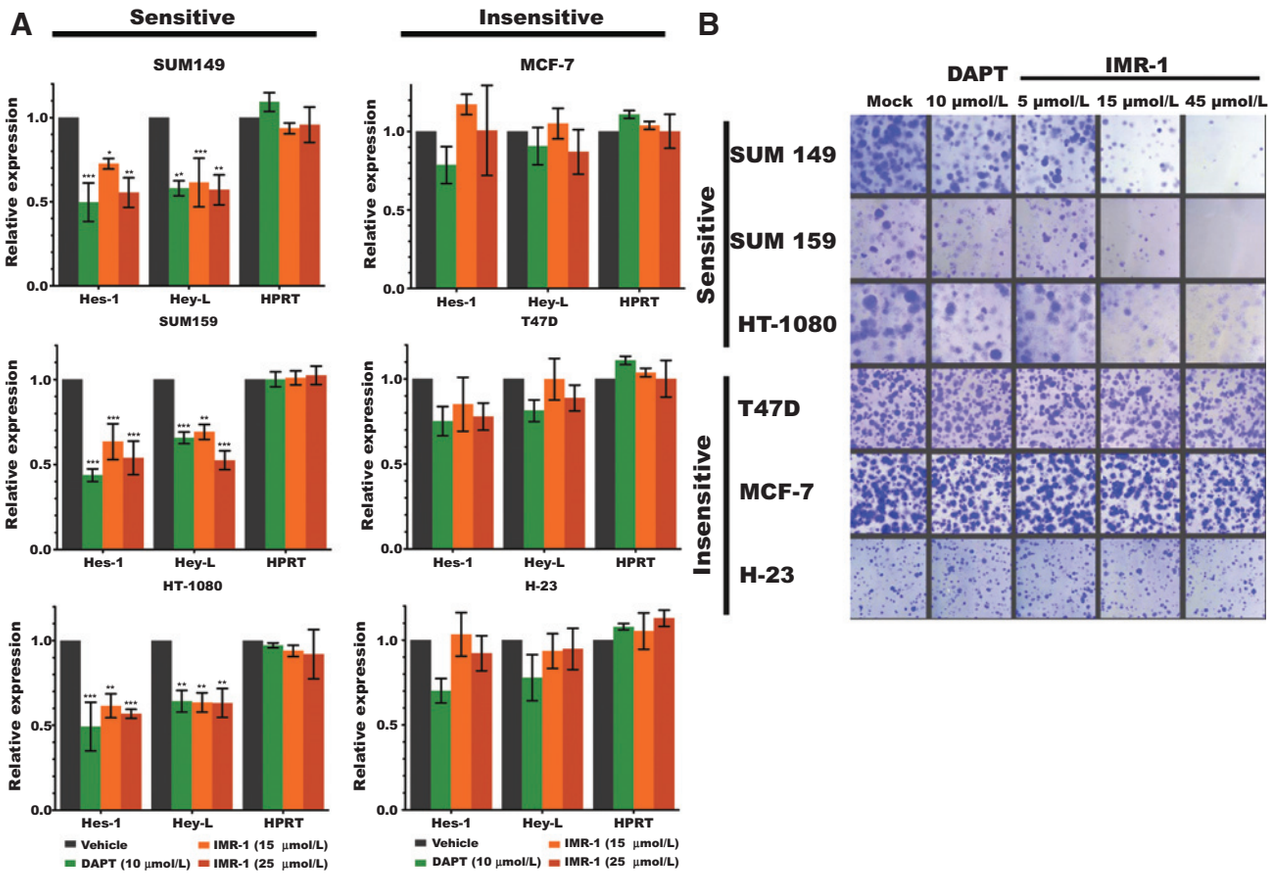

Figure 4.
IMR-1 is a specific inhibitor of the Notch pathway. A, RT-qPCR analysis on Notch-dependent (left) and Notch-independent (right) cell lines. Notch dependence is based on sensitivity to DAPT (a GSI). Relative expression of Notch target genes (*Hes-1* and *Hey-L*) compared with control (*HPRT*) is shown. B, colony formation assay on corresponding cell lines under indicated conditions compared with DMSO control.

(Supplementary Fig. S2). To further examine the effect of IMR-1 on established tumors, we utilized two independent patient-derived esophageal adenocarcinoma xenograft (PDX) models. Tumors were established in NSG mice to the size of 200 mm^3 prior to the initiation of treatment. Mice were then dosed daily via intraperitoneal injection with either IMR-1 (15 mg/kg) or DAPT (20 mg/kg) and compared with DMSO (control). Treatment of both PDX tumors with IMR-1 significantly abrogated growth to a similar level achieved with DAPT treatment (Fig. 5A and B), without any significant weight loss or other visible signs of adverse effects in the treated animals (Supplementary Fig. S3). Following 24 days of treatment, tumors were harvested and Notch target gene transcription was evaluated. These data demonstrate that treatment with IMR-1 dramatically reduced the expression level of the tested Notch target genes (Hes1, HeyL, and Notch3; Fig. 5C) in both PDX models. Similar reductions in Notch transcription were observed in DAPT-treated tumors (Fig. 5C, right). Therefore, these data demonstrate that the small-molecule IMR-1 is an inhibitor of the Notch transcriptional activation complex with demonstrated efficacy in xenograft tumor models.

IMR-1 is metabolized *in vivo* to its acid metabolite IMR-1A

In vitro studies indicate that compound IMR-1 is as a potential lead candidate for a specific Notch pathway inhibitor. Therefore, we determined the plasma pharmacokinetic profile associated with IMR-1 treatment following single intravenous and intraperitoneal dose administration in male C57 BL/6 mice (Fig. 5D). Treatment with IMR-1 did not induce any clinical signs in mice through last sample withdrawal, as evidenced by their normal appearance (data not shown). Following single intravenous and intraperitoneal administration of IMR-1 to the mice at 2 and 100 mg/kg, respectively, no signal was detected in plasma corresponding to the m/z ratio of IMR-1 at any time point. However, a signal corresponding to the m/z ratio of IMR-1A was present in the spectra, thereby the pharmacokinetic parameters of IMR-1A were determined on the basis of the parent dose (Fig. 5D) and are listed in Table 1. Following a single intravenous administration of IMR-1 at 2 mg/kg, IMR-1A exhibited low systematic plasma clearance (CL = 7 mL/min/kg) with terminal elimination half-life ($T_{1/2}$) of 2.22 hours. The normal liver blood flow in mice is 90 mL/minute/kg. In addition, the V_{ss} (volume of distribution) was approximately 4-fold higher than the normal volume of total body water (0.7 L/kg). After intraperitoneal administration of IMR-1 at 100 mg/kg dose, plasma concentrations were quantifiable up to 24 hours with T_{max} of 0.50 hours. These results indicate that IMR-1 metabolizes in plasma and its acid metabolite exhibits drug-like properties, suggesting that IMR-1 (containing an ester moiety) acts as a prodrug for IMR-1A,

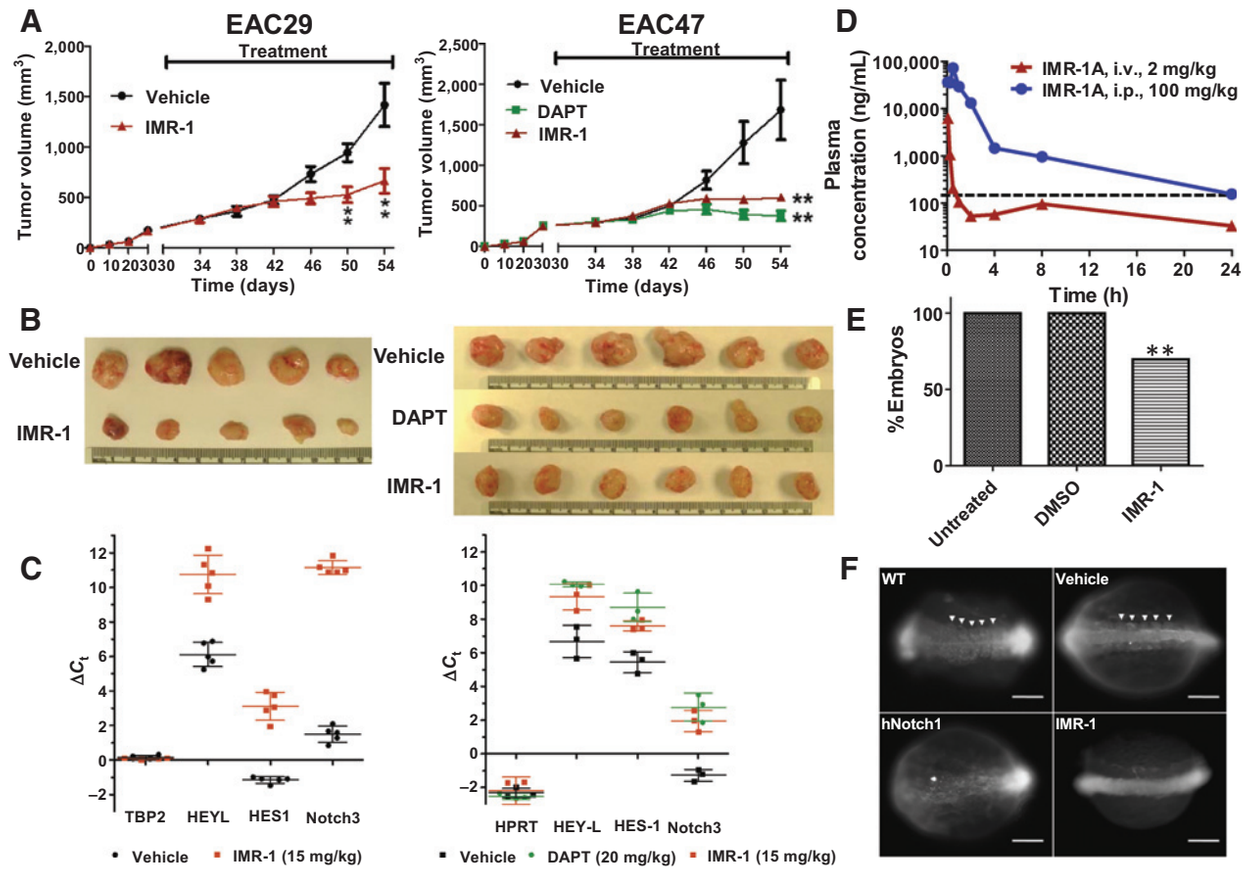

Figure 5.
IMR-1 inhibits Notch-dependent tumor growth in patient-derived xenograft models, somite development in zebrafish, and is metabolized *in vivo* to yield IMR-1A. A, tumor volume over time upon treatment (treatment for 24 days) of two independently derived esophageal adenocarcinoma PDX models (EAC29 and EAC47) with DMSO (vehicle), IMR-1 (15 mg/kg; EAC29, left), or DAPT (20 mg/kg; EAC47, right). Treatment was initiated on day 2 following transplantation of cells. Data are displayed as averages (EAC29, $n = 5$; EAC47 $n = 6$) and standard error of the mean. Unpaired two-tailed *t*-test was used to determine significance (**, $P = 0.01$). B, size of excised tumors. C, RT-qPCR analysis of Notch target genes (*HeyL*, *Hes1*, and *Notch3*) from excised tumors. *TBP* (left) and *HPRT* (right) are used as internal controls and display no change in expression upon treatment. D, plasma pharmacokinetic profile determined for the acid metabolite of IMR-1, IMR-1A, upon intravenous (2 mg/kg) and intraperitoneal (100 mg/kg) treatment of mice with IMR-1. The dashed line represents efficacy line considering an IC_{50} of 500 nmol/L. E, percentage of embryos with somites. **, $P < 0.0001$ by Fisher exact test between both untreated and drug-treated embryos and DMSO and drug-treated embryos. F, somite formation in zebrafish is sensitive to perturbations in Notch signaling. Coronal view of 13 hpf zebrafish exposed to IMR-1 at 8 hpf. Anterior to the left. Arrowheads, somites. Negative controls are WT (untreated) and vehicle (DMSO). Positive control is hNotch1 (human Notch1 intracellular domain) mRNA (100 pg)–injected embryos. Scale bar represents 0.1 mm.

most likely by increasing the solubility and cell permeability of IMR-1A.

IMR-1 inhibits Notch-dependent somite development in zebrafish

The effects of IMR-1 *in vivo* were also investigated using *D. rerio* (zebrafish). Notch signaling plays a critical role in somite formation in developing vertebrate embryos, and changes in levels of Notch signaling during development result in disruption of the symmetric, bilaterally formed somites that can be readily observed in the zebrafish embryo (Fig. 5E and F; refs. 37, 41–43). Thus, disruption of somitogenesis in zebrafish represents a convenient dose-sensitive readout for Notch pathway stimulation or inhibition. The data indicate that injecting 100 pg *hNotch1* mRNA results in defects in somitogenesis in 90% of the embryos (compared to 0% disrupted embryos in control injected animals; Fig. 5E). Disruption of somite formation was observed in 69.7% of embryos soaked in 40 μmol/L IMR-1 (Fig. 5E),

Table 1. Plasma pharmacokinetic profile determined for IMR-1A in mice upon treatment with IMR-1

Compound	Route	Dose (mg/kg)	T_{max} (h)	$T_{1/2}$ (h)	CL (mL/min/kg)
IMR-1	i.v.	2	–	NC	NC
	i.p.	100	NC	NC	–
IMR-1A	i.v.	2	–	2.22	10.33
	i.p.	100	0.50	6.16	–

NOTE: IMR-1 was administered in C57BL/6 mice via intraperitoneal (i.p.) or intravenous (i.v.) route.
Abbreviation: NC, not calculated.

consistent with alteration in Notch signaling. However, no effect was observed in embryos soaked in DMSO vehicle (control; Fig. 5E and F). These results support the role of IMR-1 as a small-molecule inhibitor of Notch signaling *in vivo*.

Discussion

Precision medicine will likely be combinatorial, as is the case for the HIV paradigm of HAART, where "class action" combinations [targeting distinct viral proteins (classes) in combination] serve to keep viral loads at a minimal level, whereas therapeutic depth with respect to the targets improves durability (44–46). Similarly, in cancer it is well accepted that there are distinct "hallmarks" of cancer physiology and that a "class action" approach may provide the best way forward for improved efficacy and durability in cancer treatment (47, 48). Therefore, there exists an urgency to identify and develop novel therapeutics to provide a comprehensive array of target-specific drugs.

There are several features of the Notch pathway mechanism that make it an attractive target for cancer therapeutics. Therefore, inhibition of complex assembly represents an attractive node for therapeutic intervention. However, to date there are no small-molecule inhibitors directly targeting the Notch intracellular pathway, which could provide greater specificity for Notch pathway inhibition. To identify inhibitors of the Notch intracellular pathway that directly target the NTC, we used CADD in combination with a novel *in vitro* assay that quantitatively measures the formation of the NTC. Cell-based assays were used to screen inhibitors with promising NTC inhibition effects and prioritize compounds for further studies, which led to the identification of IMR-1 as a potential small-molecule inhibitor of the Notch transcriptional activation complex. Herein, we demonstrate that IMR-1 prevents the recruitment of Maml1, therefore uncoupling the Notch-mediated transcriptional cascade in response to activation.

A range of experimental data indicates that IMR-1 is a *bona fide* candidate for consideration as an antineoplastic agent that targets Notch. The compound specifically inhibits the binding of Maml1 to the DNA-bound complex, selectively inhibits cell growth in cell lines that are dependent on Notch signaling for viability and affects transcription in Notch target genes, indicating IMR-1 acts on the Notch pathway through on-target effects. Furthermore, ChIP data suggest that IMR-1 functions with a mode of action distinct from the GSI DAPT to block Maml1 recruitment to the NTC. Specific inhibition of Notch-dependent activity also occurs *in vivo*. The plasma pharmacokinetic profile upon treatment with IMR-1 (ester) and the 50-fold higher potency observed for IMR-1A (acid metabolite of IMR-1) with respect to IMR-1 suggest that IMR-1 acts as a prodrug of IMR-1A. The ester moiety is commonly used in medicinal chemistry for the design of prodrugs to increase lipophilicity of polar or ionizable functionalities, such as carboxyl groups, resulting in increased cell permeability of the drug (49, 50). Furthermore, SPR data demonstrate that two arginine residues (R2061 and R2071) found in the ANK domain of Notch1 mediate binding between IMR-1 and Notch1, which confirms binding to the target and the critical importance of these two arginine residues.

The core molecular scaffold of compound IMR-1 is a thiazolidinone. Thiazolidinones are heterocyclic compounds that contain a rhodanine moiety. Many thiazolidinones have had success in the clinic. However, there are perceived liabilities related to the rhodanine moiety in drug discovery and development because rhodanines may lead to nonspecific interactions because of its potential reactivity, thus rhodanines have been referred as pan-assay interference (PAIN) molecules (51, 52). Although there is a general concern about the potential promiscuity and reactivity of this moiety, many studies have suggested that these concerns are more relevant at screening concentrations and that a comprehensive characterization of their interaction with the target should be performed, including biophysical characterization before prioritizing such compounds (53). Given the specificity of IMR-1 observed experimentally, we conclude that issues related with reactivity and nonspecific effects are not occurring since: (i) The data indicate that not all IMR-1 analogues (containing a rhodanine moiety), inhibit assembly of the NTC as exemplified by inactive compounds exhibiting no effect in the *in vitro* NTC assay (i.e., compound 1-134-22). (ii) SPR data demonstrate reversible (noncovalent) binding of IMR-1 to Notch1, and a similar profile was observed for its analogues. (iii) IMR-1 show specificity for Notch target genes and (iv) no general toxicity was observed upon *in vivo* treatment with IMR-1.

In summary, this study provides proof-of-principle for targeting the Notch transcriptional activation complex to inhibit Notch activity and presents a novel class of Notch inhibitors with the potential to be developed into therapeutic agents for the treatment of cancer. This class of inhibitors may fulfill an unmet need in terms of therapeutic agents targeting the Notch signaling pathway, providing specific inhibition of the Notch transcriptional activation complex, which could complement and/or offer an alternative to current therapeutic approaches and therefore fulfill a basic tenet of the precision medicine strategy.

Disclosure of Potential Conflicts of Interest

D. Orton is a Director of Medicinal Chemistry at StemSynergy Therapeutics, Inc. and has ownership interest in a StemSynergy Therapeutics, Inc. E. Lee is a Founder/Director at StemSynergy Therapeutics Inc.; and has ownership interest in a StemSynergy Therapeutics, Inc. D.J. Robbins is a Director at StemSynergy Therapeutics, Inc. A.J. Capobianco is a founder/Director at StemSynergy Therapeutics Inc. No potential conflicts of interest were disclosed by the other authors.

Authors' Contributions

Conception and design: L. Astudillo, T.G. Da Silva, Z. Wang, J. VanWye, T. Oashi, L.R. Neitzel, A.D. MacKerell, A.J. Capobianco

Development of methodology: L. Astudillo, T.G. Da Silva, Z. Wang, K. Jin, J. VanWye, X. Zhu, P.E.M. Lopes, L.R. Neitzel, E. Lee, A.D. MacKerell, A.J. Capobianco

Acquisition of data (provided animals, acquired and managed patients, provided facilities, etc.): L. Astudillo, T.G. Da Silva, X. Han, K. Jin, J. VanWye, X. Zhu, K. Weaver, T. Oashi, P.E.M. Lopes, L.R. Neitzel, E. Lee, A.D. MacKerell

Analysis and interpretation of data (e.g., statistical analysis, biostatistics, computational analysis): L. Astudillo, T.G. Da Silva, Z. Wang, X. Han, K. Jin, J. VanWye, X. Zhu, T. Oashi, P.E.M. Lopes, L.R. Neitzel, R. Landgraf, D.J. Robbins, A.D. MacKerell, A.J. Capobianco

Writing, review, and/or revision of the manuscript: L. Astudillo, T.G. Da Silva, X. Zhu, D. Orton, A.D. MacKerell, A.J. Capobianco

Administrative, technical, or material support (i.e., reporting or organizing data, constructing databases): Z. Wang, J. VanWye, T. Oashi, A.J. Capobianco

Study supervision: A.J. Capobianco

Acknowledgments

The authors thank members of the Capobianco and Robbins laboratory and the University of Maryland Computer-Aided Drug Design Center for support and technical assistance.

Grant Support

This work was supported by the NCI (NCI R01CA083736-12A1, NCI R01CA125044-02 to A.J. Capobianco), the NIH (R01GM081635 and R01GM103926 to E. Lee), the Training Program in Stem Cell and Regenerative Developmental Biology (T32HD007502 to L.R. Neitzel), Samuel Waxman Cancer Research Foundation (A.J. Capobianco and A.D. MacKerell), and the UM/Sylvester Braman Family Breast Cancer Institute's Women's Cancer League Developmental Grant (A.J. Capobianco). This project was also generously supported by funding from the Dewitt Daughtry Family Department of Surgery and the Sylvester Comprehensive Cancer Center (A.J. Capobianco).

The costs of publication of this article were defrayed in part by the payment of page charges. This article must therefore be hereby marked *advertisement* in accordance with 18 U.S.C. Section 1734 solely to indicate this fact.

Received January 12, 2016; revised March 23, 2016; accepted March 30, 2016; published OnlineFirst April 13, 2016.

References

1. Hoppe PE, Greenspan RJ. Local function of the NOTCH gene for embryonic ectodermal pathway choice in Drosophila. Cell 1986;46:773–83.
2. Artavanis-Tsakonas S, Rand MD, Lake RJ. Notch signaling: cell fate control and signal integration in development. Science 1999;284:770–6.
3. Sander GR, Powell BC. Expression of notch receptors and ligands in the adult gut. J Histochem Cytochem 2004;52:509–16.
4. Stump G, Durrer A, Klein A-L, Lütolf S, Suter U, Taylor V. Notch1 and its ligands Delta-like and Jagged are expressed and active in distinct cell populations in the postnatal mouse brain. Mech Dev 2002;114:153–9.
5. Ranganathan P, Weaver KL, Capobianco AJ. Notch signaling in solid tumours: a little bit of everything but not all the time. Nat Rev Cancer 2011;11:338–51.
6. Koch U, Radtke F. Notch and cancer: a double-edged sword. Cell Mol Life Sci 2007;64:2746–62.
7. Radtke F, Raj K. The role of Notch in tumorigenesis: oncogene or tumour suppressor? Nat Rev Cancer 2003;3:756–67.
8. Wang J, Sullenger BA, Rich JN. Notch signaling in cancer stem cells. Adv Exp Med Biol 2012;727:174–85.
9. Espinoza I, Pochampally R, Xing F, Watabe K, Miele L. Notch signaling: targeting cancer stem cells and epithelial-to-mesenchymal transition. Onco Targets Ther 2013;6:1249–59.
10. Tamura K, Taniguchi Y, Minoguchi S, Sakai T, Tun T, Furukawa T, et al. Physical interaction between a novel domain of the receptor Notch and the transcription factor RBP-J kappa/Su(H). Curr Biol 1995;5:1416–23.
11. Aster JC, Robertson ES, Hasserjian RP, Turner JR, Kieff E, Sklar J. Oncogenic forms of NOTCH1 lacking either the primary binding site for RBP-J kappa or nuclear localization sequences retain the ability to associate with RBP-J kappa and activate transcription. J Biol Chem 1997;272:11336–43.
12. Nam Y, Sliz P, Song LY, Aster JC, Blacklow SC. Structural basis for cooperativity in recruitment of MAML coactivators to Notch transcription complexes. Cell 2006;124:973–83.
13. Jeffries S, Robbins DJ, Capobianco AJ. Characterization of a high-molecular-weight Notch complex in the nucleus of Notch(ic)-transformed RKE cells and in a human T-cell leukemia cell line. Mol Cell Biol 2002;22:3927–41.
14. Wilson JJ, Kovall RA. Crystal structure of the CSL-Notch-Mastermind ternary complex bound to DNA. Cell 2006;124:985–96.
15. Tiyanont K, Wales TE, Siebel CW, Engen JR, Blacklow SC. Insights into Notch3 activation and inhibition mediated by antibodies directed against its negative regulatory region. J Mol Biol 2013;425:3192–204.
16. Takebe N, Nguyen D, Yang SX. Targeting notch signaling pathway in cancer: clinical development advances and challenges. Pharmacol Ther 2014;141:140–9.
17. Sharma A, Paranjape AN, Rangarajan A, Dighe RR. A monoclonal antibody against human Notch1 ligand-binding domain depletes subpopulation of putative breast cancer stem-like cells. Mol Cancer Ther 2012;11:77–86.
18. Fischer M, Yen W-C, Kapoun AM, Wang M, O'Young G, Lewicki J, et al. Anti-DLL4 inhibits growth and reduces tumor-initiating cell frequency in colorectal tumors with oncogenic KRAS mutations. Cancer Res 2011;71:1520–5.
19. Berezovska O, Jack C, McLean P, Aster JC, Hicks C, Xia W, et al. Aspartate mutations in presenilin and gamma-secretase inhibitors both impair notch1 proteolysis and nuclear translocation with relative preservation of notch1 signaling. J Neurochem 2000;75:583–93.
20. Shih I-M, Wang T-L. Notch signaling, gamma-secretase inhibitors, and cancer therapy. Cancer Res 2007;67:1879–82.
21. De Kloe GE, De Strooper B. Small molecules that inhibit Notch signaling. Methods Mol Biol 2014;1187:311–22.
22. Alves-Guerra M-C, Ronchini C, Capobianco AJ. Mastermind-like 1 is a specific coactivator of beta-catenin transcription activation and is essential for colon carcinoma cell survival. Cancer Res 2007;67:8690–8.
23. Maillard I, Weng AP, Carpenter AC, Rodriguez CG, Sai H, Xu L, et al. Mastermind critically regulates Notch-mediated lymphoid cell fate decisions. Blood 2004;104:1696–702.
24. Helms W, Lee H, Ammerman M, Parks AL, Muskavitch MA, Yedvobnick B. Engineered truncations in the *Drosophila* mastermind protein disrupt Notch pathway function. Dev Biol 1999;215:358–74.
25. Wu L, Aster JC, Blacklow SC, Lake R, Artavanis-Tsakonas S, Griffin JD. MAML1, a human homologue of *Drosophila* mastermind, is a transcriptional co-activator for NOTCH receptors. Nat Genet 2000;26:484–9.
26. Kankel MW, Hurlbut GD, Upadhyay G, Yajnik V, Yedvobnick B, Artavanis-Tsakonas S. Investigating the genetic circuitry of mastermind in *Drosophila*, a notch signal effector. Genetics 2007;177:2493–505.
27. Moellering RE, Cornejo M, Davis TN, Del Bianco C, Aster JC, Blacklow SC, et al. Direct inhibition of the NOTCH transcription factor complex. Nature 2009;462:182–8.
28. Weaver KL, Alves-Guerra M-C, Jin K, Wang Z, Han X, Ranganathan P, et al. NACK is an integral component of the Notch transcriptional activation complex and is critical for development and tumorigenesis. Cancer Res 2014;74:4741–51.
29. Drescher DG, Ramakrishnan NA, Drescher MJ. Surface plasmon resonance (SPR) analysis of binding interactions of proteins in inner-ear sensory epithelia. Methods Mol Biol 2009;493:323–43.
30. Heitjan DF, Manni A, Santen RJ. Statistical analysis of in vivo tumor growth experiments. Cancer Res 1993;53:6042–50.
31. Kovall RA. More complicated than it looks: assembly of Notch pathway transcription complexes. Oncogene 2008;27:5099–109.
32. Vasquez-Del Carpio R, Kaplan FM, Weaver KL, VanWye JD, Alves-Guerra M-C, Robbins DJ, et al. Assembly of a notch transcriptional activation complex requires multimerization. Mol Cell Biol 2011;31:1396–408.
33. Choi SH, Wales TE, Nam Y, O'Donovan DJ, Sliz P, Engen JR, et al. Conformational locking upon cooperative assembly of notch transcription complexes. Structure 2012;20:340–9.
34. Zhong S, MacKerell ADJr. Binding response: a descriptor for selecting ligand binding site on protein surfaces. J Chem Inf Model 2007;47:2303–15.
35. Kuntz ID, Blaney JM, Oatley SJ, Langridge R, Ferrin TE. A geometric approach to macromolecule-ligand interactions. J Mol Biol 1982;161:269–88.
36. Oashi T, Ringer AL, Raman EP, MacKerell ADJr. Automated selection of compounds with physicochemical properties to maximize bioavailability and druglikeness. J Chem Inf Model 2011;51:148–58.
37. Kageyama R, Niwa Y, Isomura A, González A, Harima Y. Oscillatory gene expression and somitogenesis. Wiley Interdiscip Rev Dev Biol 2012;1:629–41.
38. Macias AT, Mia MY, Xia GJ, Hayashi J, MacKerell AD. Lead validation and SAR development via chemical similarity searching: application to compounds targeting the pY+3 site of the SH2 domain of p56(lck). J Chem Inf Model 2005;45:1759–66.
39. Williams FM. Clinical significance of esterases in man. Clin Pharmacokinet 1985;10:392–403.
40. Wang Z, Da Silva TG, Jin K, Han X, Ranganathan P, Zhu X, et al. Notch signaling drives stemness and tumorigenicity of esophageal adenocarcinoma. Cancer Res 2014;74:6364–74.
41. Soza-Ried C, Öztürk E, Ish-Horowicz D, Lewis J. Pulses of Notch activation synchronise oscillating somite cells and entrain the zebrafish segmentation clock. Development 2014;141:1780–8.

42. Lewis J, Hanisch A, Holder M. Notch signaling, the segmentation clock, and the patterning of vertebrate somites. J Biol 2009;8:44.
43. Fongang B, Kudlicki A. The precise timeline of transcriptional regulation reveals causation in mouse somitogenesis network. BMC Dev Biol 2013;13:42.
44. DeVita VT, Eggermont AMM, Hellman S, Kerr DJ. Clinical cancer research: the past, present and the future. Nat Rev Clin Oncol 2014;11: 663–9.
45. Srinivasa S, Grinspoon SK. Metabolic and body composition effects of newer antiretrovirals in HIV-infected patients. Eur J Endocrinol 2014;170: R185–202.
46. Du W, Elemento O. Cancer systems biology: embracing complexity to develop better anticancer therapeutic strategies. Oncogene 2014;34: 3215–25.
47. Hanahan D, Weinberg RA. The hallmarks of cancer. Cell 2000;100:57–70.
48. Lazebnik Y. What are the hallmarks of cancer? Nat Rev Cancer 2010;10:232–3.
49. Rautio J, Kumpulainen H, Heimbach T, Oliyai R, Oh D, Järvinen T, et al. Prodrugs: design and clinical applications. Nat Rev Drug Discov 2008;7: 255–70.
50. Huttunen KM, Raunio H, Rautio J. Prodrugs—from serendipity to rational design. Pharmacol Rev 2011;63:750–71.
51. Baell JB. Observations on screening-based research and some concerning trends in the literature. Future Med Chem 2010;2:1529–46.
52. Tomašić T, Peterlin Mašič L. Rhodanine as a scaffold in drug discovery: a critical review of its biological activities and mechanisms of target modulation. Expert Opin Drug Discov 2012;7:549–60.
53. Mendgen T, Steuer C, Klein CD. Privileged scaffolds or promiscuous binders: a comparative study on rhodanines and related heterocycles in medicinal chemistry. J Med Chem 2012;55:743–53.